PERGAMON

Vision Research 41 (2001) 3883–3902

Vision Research

www.elsevier.com/locate/visres

Attention-dependent brief adaptation to contour orientation: a high-level aftereffect for convexity?

Satoru Suzuki *

Department of Psychology, Northwestern University, 2029 Sheridan Rd., Evanston, IL 60208, USA

Received 31 July 2000; received in revised form 17 August 2001

Abstract

In contrast to the abundant literature investigating how orientation coding depends on edges defined by various image features, relatively little is known about how coding of orientation might also depend on the two distinct functional roles that oriented edges commonly play. Oriented lines can delineate outline contours of a figure or they can form texture. The results of five experiments using orientation aftereffects measured with brief tests (27 ms, backward masked; adapt-to-test interval = 201 ms) provided evidence that brief stimuli (< 135 ms) selectively adapt coding of contour-line orientation rather than coding of line-texture orientation. Furthermore, parametric results revealed that the rapidly adapting aftereffects for contour orientation are characterized by (1) broad orientation tuning (peaking at $\pm 30°$ to $\pm 50°$ from test orientation), (2) indifference as to how the contours are defined (e.g. bright lines, high-pass-filtered lines, faint lines generated by the spatial inhomogeneity of visual sensitivity), (3) rapid saturation at low contrast energy, (4) strong modulation by selective attention, and (5) relative size tolerance. These characteristics appear to parallel those of cells in the high end of the visual form processing pathway (such as inferotemporal cortex). It is thus suggested that the rapidly adapting contour orientation aftereffects reported here may be mediated by high-level neural units that encode global configurations of orientation (e.g. convexity and concavity).

Keywords: Adaptation; Aftereffect; Attention; Contour; Orientation; Size; Texture

1. Introduction

Staring at an oriented bar (or a grating) for a period of time makes a subsequently presented bar (or a grating) with a slightly shifted orientation appear tilted further away from the adapted orientation—a tilt aftereffect (e.g. Gibson & Radner, 1938). To a first approximation, these so-called "direct" tilt aftereffects are thought to be mediated by activation-based suppressive gain control (e.g. Wilson & Humanski, 1993; Sclar, Lennie, & DePriest, 1989; Ohzawa, Sclar, & Freeman, 1985) of orientation-tuned neurons. For example, in the primary visual cortex (V1), response suppression in a cell tends to be strong following that cell's preferred stimulus, but nearly absent following a null stimulus that hardly excites the cell (e.g. Saul & Cynader, 1989; Bonds, 1991; Carandini, Movshon, & Ferster, 1998). In explaining tilt aftereffects, it is commonly assumed that perceived orientation is determined by a central-tendency statistic (such as the centroid; e.g. Lee, Rohrer, & Sparks, 1988) of the response distribution of a population of cells tuned to different orientations. When adapting and test orientations are close, that is, when the test orientation is within the orientation-tuning ranges of the adapted cells, cells tuned to the adapted side of the test orientation respond weakly to the test orientation (because of suppression) relative to cells tuned to the non-adapted side of the test orientation. Such a lopsided population response leaning away from the adapted orientation would make the test orientation appear tilted away from the adapted orientation[1] (see Braddick, Campbell, & Atkinson, 1978, for a textbook example).

* Tel.: +1-847-467-1271; fax: +1-847-673-9685.
E-mail address: satoru@northwestern.edu (S. Suzuki).

[1] This traditional account of tilt aftereffects is illustrative but overly simplistic. For example, Meese and Georgeson (1996) suggested that perceived orientation is coded following various stages of image transformation that preserve local-global image coherence by maximizing the overall contrast energy.

0042-6989/01/$ - see front matter
PII: S0042-6989(01)00249-8

Assuming that tilt aftereffects are direct perceptual consequences of adaptation of neural units involved in population coding of orientation, researchers have used these phenomena to understand how the visual system codes orientation of edges defined by different image features. Tilt aftereffects have been demonstrated using a bar (or a grating) defined by a variety of image features: luminance contrast (e.g. Mitchell & Muir, 1976; Campbell & Maffei, 1971), color contrast (e.g. Held, Shattuck-Hufnagel, & Moskowitz, 1982; Held & Shattuck, 1971; Flanagan, Cavanagh, & Favreau, 1990), binocular disparity (e.g. Tyler, 1975; Wolfe & Held, 1982), subjective contours (e.g. Paradiso, Shimojo, & Nakayama, 1989; van der Zwan & Wenderoth, 1995; Berkley, Debruyn, & Orban, 1994), and motion contrast (e.g. Berkley et al., 1994). Demonstrations of cross-attribute tilt aftereffects (e.g. adaptation to a luminance-, subjective-contour-, or motion-defined grating producing tilt aftereffects on a grating defined by the same or a different attribute; Berkeley et al., 1994; Paradiso et al., 1989) suggest that neural adaptation underlying tilt aftereffects is mediated by cells that respond to their preferred orientations regardless of how the stimulus is defined. A small proportion of cells in the inferotemporal cortex (IT) exhibit equivalent orientation tunings (preferences and tuning widths) for bars defined by luminance, texture, and motion (e.g. Sary, Vogels, Kovacs, & Orban, 1995). A subset of V2 cells shows similar orientation preferences for bars defined by luminance and subjective contours (e.g. Peterhans, von der Heydt, & Baumgartner, 1986; Peterhans & von der Heydt, 1991; Sheth, Sharma, Rao, & Sur, 1996), or for bars defined by multiple attributes such as luminance, dot-density, and motion, as well as subjective contours (e.g. Leventhal, Wang, Schmolesky, & Zhou, 1998). Even in V1 some cells respond to a subclass of subjective contours (e.g. Grosof, Shapley, & Hawken, 1993; Sheth et al., 1996; though it has been shown that ensemble activity of V1 cells is correlated with perception of texture- and motion-defined regions, it is unknown as to whether such ensemble activity encodes orientation of contours defined by these attributes; e.g. Lamme, Van Dijk, & Spekreijse, 1993a,b).

Whereas demonstrations of cross-attribute tilt aftereffects imply the existence of attribute-invariant coding of orientation (perhaps mediated by cells in V2 through IT), reports of attribute-specific tilt aftereffects suggest that orientation coding occurs at multiple neural loci which are individually capable of producing tilt aftereffects. For example, tilt aftereffects can be color specific; following alternate adaptation to gratings defined by two different color contrasts, one tilted clockwise and the other tilted counter-clockwise relative to the test orientation, opposite tilt aftereffects can be induced to the test stimuli of the respective adaptation colors (e.g. Held et al., 1982; Held & Shattuck, 1971; Flanagan et al., 1990). These results suggest that orientation is coded independently by different groups of orientation-tuned cells that are also selective for different colors. Cells with these properties have been reported in V1 (peri-blob regions; e.g. Ts'o & Gilbert, 1988), V2 (e.g. Ts'o & Roe, 1995), and V4 (e.g. Desimone & Schein, 1987). In addition, the fact that luminance-defined stimuli produce tilt aftereffects that are tuned for spatial frequency (e.g. Ware & Mitchell, 1974; Held et al., 1982) is consistent with the fact that responses of V1 neurons (and some V2 and V4 neurons as well) are tuned for both spatial frequency and orientation (e.g. Hubel & Wiesel, 1968; De Valois, Albrecht, & Thorell, 1982; Foster, Gaska, Nagler, & Polen, 1985; Desimone & Schein, 1987).

Previous research thus suggests that edge orientation is coded at both attribute-invariant and attribute-specific levels of image processing, concurrently in multiple visual cortical areas. In contrast to the abundance of literature investigating how coding of orientation depends on edges defined by various image features, relatively little is known about how coding of orientation might also depend on the two distinct functional roles that oriented edges commonly play. Oriented lines can delineate outline contours of a figure or they can form texture. For example, in Fig. 1a, the oriented lines mark the outline contours of the hourglass and diamond shapes. In Fig. 1b, the oriented lines form the square patches of texture; although the line textures are tilted, the outline contours of the texture patches are vertical and horizontal.

Previous studies using single lines (e.g. Magnussen & Kurtenbach, 1980; O'Shea, Wilson, & Duckett, 1993) and gratings (e.g. Mitchell & Muir, 1976; Campbell & Maffei, 1971) generally produced similar angular tuning of tilt aftereffects (maximum when the angular difference between the adaptor and the test stimulus is about $\pm 15°$). These results seem to suggest that the coding of orientation underlying tilt aftereffects is similar for a single line and for a grating (line texture). However, an isolated line segment is a rather extreme case of an outline contour. Moreover, tilt aftereffects induced by outline contours and line textures have never been compared rigorously within a single study.

Furthermore, since an important goal of the initial stage of visual processing is to determine object orientation, the visual system may code orientation of outline contours rapidly, and separately from orientation of line textures. If so, brief stimuli might selectively adapt coding of contour orientation, producing strong contour-orientation based aftereffects, without affecting coding of line-texture orientation, producing little texture-orientation based aftereffects. The use of brief

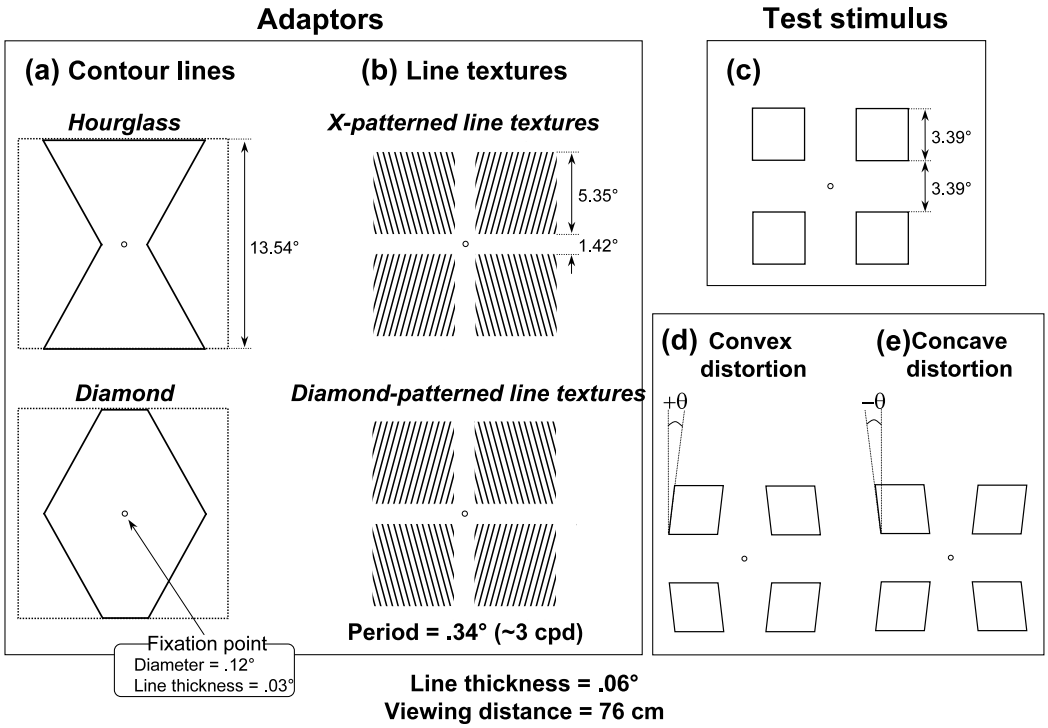

Fig. 1. The adaptors and the test stimulus used in the experiments. (a) The contour-line adaptors—the oriented lines form the outline contours of the hourglass and the diamond figures; the figures were drawn to fit within the square boxes indicated by the dotted lines for all contour angles. (b) The line-texture adaptors—the oriented lines form square patches of texture. (c) The test stimulus—a square array of four squares—used to measure the orientation aftereffect. The aftereffects were measured as shape-distortion effects induced on the test stimulus. (d) A convex distortion is induced by the hourglass figure and the X-patterned line textures under appropriate conditions. (e) A concave distortion is induced by the diamond figure and the diamond-patterned line textures under appropriate conditions. In subsequent graphs, positive values of θ are used to indicate degrees of induced convexity (d), whereas negative values of θ are used to indicate degrees of induced concavity (e). Dimensions indicate degrees of visual angle.

adaptation is also motivated by recent studies by Suzuki and colleagues suggesting that brief stimuli selectively adapt high-level shape representations (e.g. Suzuki & Cavanagh, 1998; Suzuki & Rivest, 1998; Rivest, Intriligator, Warner, & Suzuki, 1997; Rivest, Intriligator, Suzuki, & Warner, 1998; Suzuki, 1999).

Orientation aftereffects were measured in terms of a shape-distortion effect, that is, the apparent convexity and concavity induced on a briefly presented square array of four smaller squares (Fig. 1c; also used in Suzuki, 1999). The outline-contour stimulus used for adaptation was either an hourglass figure (Fig. 1a, top) or a diamond figure (Fig. 1a, bottom). The hourglass figure tends to induce a convex distortion on the test array (Fig. 1d), whereas the diamond figure tends to induce a concave distortion on the test array (Fig. 1e) under appropriate conditions. The line-texture stimulus used for adaptation consisted of a square array of four texture patches (Fig. 1b). The line textures were arranged such that they globally formed either an X-shaped pattern (Fig. 1b, top) or a diamond-shaped pattern (Fig. 1b, bottom). The X-patterned textures tend to induce a convex distortion on the test array (Fig. 1d), whereas the diamond-patterned textures tend to induce a concave distortion on the test array (Fig. 1e) under appropriate conditions. By measuring tilt aftereffects as a shape-distortion effect (rather than as induced tilt relative to perceived vertical), potential contributions of non-visual factors such as gravity (e.g. Wolfe & Held, 1982) were avoided. It is also known that people demonstrate high acuity for convex/concave discriminations (e.g. Rubin, Nakayama, & Shapley, 1996). The test squares (Fig. 1c) were briefly flashed (and backward masked) because previous studies demonstrated that brief tests produce larger tilt aftereffects (e.g. Wolfe, 1984) as well as other visual distortion illusions (e.g. Suzuki & Cavanagh, 1997, 1998).

The results of five experiments are reported. The main hypothesis that brief stimuli might selectively adapt a mechanism that encodes contour-line orientation rather than line-texture orientation, was tested (and supported) in Experiments 1A, 1B, and 2. In Experiments 3A and 3B, attentional modulation of the rapidly adapting contour-orientation aftereffects was examined by using overlapping adaptors (the hourglass and the diamond). Experiment 3B examined the possibility that these aftereffects induced by the hourglass and the diamond contours are global shape aftereffects

rather than the sum of local orientation aftereffects. In the general discussion, the overall parametric characteristics of the contour-orientation aftereffects (dependencies on adaptation angle, spatial frequency, contrast energy, selective attention, and size) will be compared with the known response characteristics of high-level visual neurons in the ventral visual stream. It will be suggested that brief presentations of the hourglass and the diamond contours selectively adapt a high-level shape-processing mechanism tuned to overall convexity and concavity.

2. General method

The experiments were conducted in a light-adapted condition. The author, SS, and two naïve observers, YS and ET, (all experienced psychophysical observers) participated in all or some of the experiments. All had normal or corrected-to-normal vision (SS with corrective glasses, ET with contact lenses, and YS without any correction). Stimuli were shown on a 17-inch color monitor (75 Hz) and the experiments were controlled by a Macintosh PowerMac 8600/300MHz with Vision Shell software (Micro ML, Quebec, Canada).

A trial began with a warning beep and a presentation of a blank fixation screen (112 cd/m^2) with a small gray fixation circle in the middle (Fig. 2). After 1342 ms, an adaptor was presented for a variable duration (27, 134, or 2684 ms). The adaptor (outline figure—hourglass or diamond, or line textures—X-patterned or diamond-patterned) was drawn with bright lines (width = 0.06°, variable luminance) against a dark background (3.8 cd/m^2). Following a 201 ms return of the blank fixation screen, the high-contrast test stimulus (dark, 3.8 cd/m^2, against a bright, 112 cd/m^2, background; contrast = -0.94 computed as $[L_{\text{line}} - L_{\text{background}}]/[L_{\text{line}} + L_{\text{background}}]$) was flashed briefly (27 ms), immediately followed by a full-screen random-dot mask (403 ms; bright dots = 112 cd/m^2 and dark dots = 3.8 cd/m^2; dot size = 0.06° × 0.06°). The observer then responded that the test array appeared either convex (e.g. Fig. 1d) or concave (e.g. Fig. 1e) in a forced choice manner.

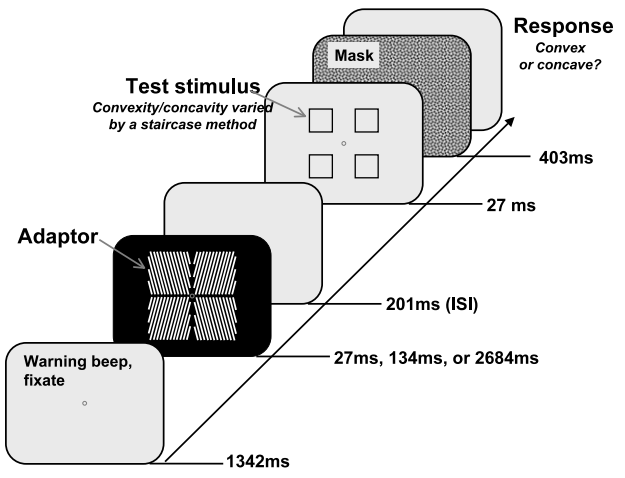

Fig. 2. Sequence of events in an experimental trial. At the end of each trial, the observer responded whether the test stimulus appeared convex or concave in a forced choice manner. A staircase procedure adjusted the orientation of the vertical lines of the test squares appropriately to cancel out the convexity/concavity induced by the aftereffects.

The adaptation display was presented in reversed contrast for two reasons: (1) to reduce any sensation of apparent motion between the adaptor and the test stimulus, and (2) to indicate to the observer when the adaptor was presented (especially when the adaptor was low contrast and flashed briefly). It has been shown that contrast-polarity reversal between the adaptor and the test stimulus little affects tilt aftereffects (e.g. O'Shea et al., 1993; Magnussen & Kurtenbach, 1979). The dimensions of the stimuli are shown in Fig. 1. The viewing distance was 76 cm. Though a chin rest was not used, the observers frequently measured and adjusted their distance from the monitor.

A staircase method was used to estimate the magnitude of the orientation aftereffect (measured as a convexity aftereffect). In most cases, two interleaved staircases alternated across trials—*double-staircase method*; one staircase started at a distinctly convex configuration of the test stimulus ($\theta = +1.91°$), whereas the other staircase started at a distinctly concave configuration ($\theta = -1.91°$); the convention (θ) used to describe the convexity and concavity is shown in Fig. 1d and e. Each "convex" response made the test stimulus in the following trial for the corresponding staircase less convex by 0.48°; similarly, each "concave" response made the test stimulus for the following trial for the corresponding staircase more convex by 0.48°. The trials were terminated when both staircases had gone through at least six reversals. The values of the last six reversals for the two staircases, 12 reversals total, were averaged to estimate the magnitude of the aftereffect (i.e. the degree of θ required to cancel the aftereffect); the *SEM* (standard error of the mean) of the reversal values was used as the error bar.[2] In a minority of cases (Experiment 1A and pilot results), a single staircase was used—*single-staircase method*; it started with a straight (neither convex nor concave)

[2] The *SEM* of the reversal values reflects variability in perceived orientation of the test figure within each run of a staircase. The random variability of aftereffects across measurements (across staircases) is reflected in the degree to which the mean reversal values obtained from individual staircases randomly fluctuated around a smooth function as the angle, the contrast, or the scale of the adaptor was systematically varied. As seen in the data, the across-measurement variability was generally small. Furthermore, all patterns of data discussed here were tested for stability by replicating at least once for observers SS and YS.

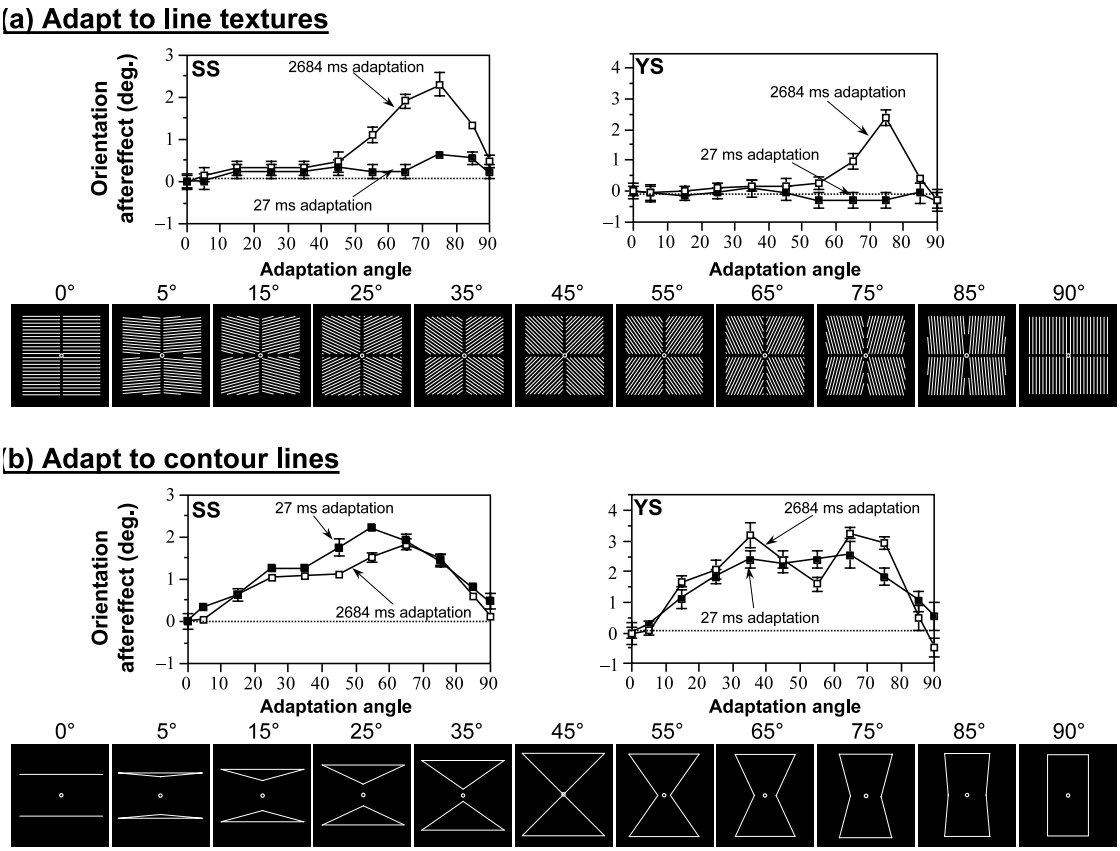

Fig. 3. The dependence of the orientation aftereffects on the adaptation angle (observers SS and YS; Experiment 1A). (a) The aftereffects obtained from 27 ms (solid symbols) and 2684 ms (open symbols) adaptation to the X-patterned line textures. (b) The aftereffects obtained from 27 ms (solid symbols) and 2684 ms (open symbols) adaptation to the hourglass figure. Also shown are schematic drawings of the adaptors corresponding to the different adaptation angles used.

configuration (Fig. 1c) and terminated after six reversals; the aftereffects were estimated by averaging over the six reversal values.

3. Experiment 1A

3.1. How do contour-orientation and texture-orientation aftereffects depend on duration and angle of adaptation?

The angle of the adaptor lines was systematically varied from 0° (horizontal) to 90° (vertical). Previous studies demonstrated that when the adaptation duration was relatively long (e.g. seconds to minutes of initial adaptation and seconds of top-up adaptation preceding each trial), direct[3] tilt aftereffects generally reached their peak magnitude when the adaptor orientation was about $\pm 15°$ from the test orientation and disappeared when the adaptor orientation reached about $\pm 40°$ to $\pm 60°$ from the test orientation (e.g. Mitchell & Muir, 1976; Campbell & Maffei, 1971; O'Shea et al., 1993; Magnussen & Kurtenbach, 1980). The aim of this experiment was to determine whether the orientation aftereffects due to the line textures and the outline contours dissociated with respect to the manipulations of adaptation angle (0° through 90°) and duration (27 versus 2684 ms). Note that long adaptation to the line-texture stimulus was similar to the conditions used in previous tilt-aftereffect studies; therefore, that condition was expected to yield a comparable angular dependence, peaking at about $\pm 15°$ from vertical.

The luminance of the adaptor was 112 cd/m^2 (contrast = 0.94; CIE[.286,.301]—white; all color guns set to maximum). For the outline-contour adaptor, the angles were varied such that the oriented parts of the contours always went through the centers of the corresponding squares of the test stimulus; the entire figure was also made to fit within the overall square region (shown in Fig. 1a with dotted lines). These constraints

[3] The global axes of symmetry for all of the stimuli used in this study were vertical and horizontal and aftereffects were measured as shape-distortion effects. Therefore, the indirect component of tilt aftereffect, which is thought to be mediated by the orientation of a global axis of symmetry (e.g. Wenderoth & van der Zwan, 1989; Wenderoth & Johnstone, 1987), was not expected to be obtained.

resulted in splitting up the figure into two triangles when the adapting angle was less than 45° (see Fig. 3 for schematic drawings).

Observers SS and YS were tested in four adaptation conditions, two types of adaptors (the X-patterned textures and the hourglass figure) crossed with two adaptation durations (27 and 2684 ms). In each condition, the aftereffect was measured using the single-staircase method. The adaptation angle was varied from horizontal (0°) through vertical (90°) in one session (test angle was vertical, 90°); a 2-min break was inserted between successive measurements of the aftereffect as the adaptation angle was changed. At least a 1-h break (typically a 1-day break) was given between adaptation conditions.

To insure the stability of the data, the four conditions were repeated for SS while the adaptation angle was swept in the reversed order (from 90° through 0°) using the double-staircase method. YS repeated the four conditions with the diamond-patterned textures and the diamond figure instead of the X-patterned textures and the hourglass figure, using the single-staircase method. These replication conditions yielded the same pattern of results as those reported.

3.2. Results and discussion

As expected, long adaptation (2684 ms) to the line textures generated the pattern of angular dependence typically reported in the previous studies of tilt aftereffects using similar conditions (peaking at 75°, i.e. $\pm 15°$ from the test orientation; Fig. 3a, open symbols). A striking finding is that the aftereffect considerably reduced (completely disappeared for YS) when adaptation to the line textures was made brief (27 ms; Fig. 3a, filled symbols). This result appears to contradict Sekuler and Littlejohn's report (1974) of reliable tilt aftereffects using a briefly presented adaptation grating (18 ms); this issue will be resolved later.

As shown in Fig. 3b, a rather different pattern of results was obtained when the hourglass contours were used as the adaptor. Unlike the line-texture case, the brief, 27 ms, adaptation (filled symbols) and the prolonged, 2684 ms, adaptation (open symbols) both produced equivalent degrees of orientation aftereffects. Furthermore, the broad angular tuning of the hourglass-contour-induced aftereffects (reliable aftereffects obtained even when the adaptation angle was $\pm 70°$ away from vertical) is in contrast with the narrow angular tuning obtained for the line-texture-induced aftereffects.

The dissociation between the line-texture aftereffect and the contour-line aftereffect, the former being narrowly tuned and requiring prolonged adaptation and the latter being broadly tuned and requiring only brief adaptation, is consistent with the idea that line textures and outline contours activate different orientation coding mechanisms. However, there are alternative ways in which at least the dramatic reduction of the line texture aftereffects with brief adaptation could be explained.

First, since the test stimulus consisted of outline squares, it might be more compatible (in terms of spatial-frequency contents) with the outline hourglass contours than with the X-patterned textures. It is possible that if the test stimulus consisted of line textures similar to the X-patterned textures, brief adaptation might then substantially reduce aftereffects induced by the hourglass contours while leaving aftereffects induced by the X-patterned textures relatively intact. This possibility was tested in the next experiment by having the four squares of the test stimulus made up of texture patches; these *grating-defined squares* consisted of bars that had the same width and spacing as the X-patterned textures (see Fig. 4 for a schematic drawing).

Second, it might be the case that the hourglass contours produced aftereffects following brief adaptation mainly because they contained more lower-spatial-frequency energy than did the X-patterned textures. It might be that orientation-tuned cells that are selective for low spatial frequencies tend to be rapidly adapting, whereas those selective for high-spatial frequencies tend to be slow adapting. This possibility was tested by filtering out low-spatial-frequency components from the hourglass contours, using a "balanced dot" technique (e.g. Durgin & Proffitt, 1996; Carlson, Moeller, & Anderson, 1984); the white contours of the hourglass figure were sandwiched between a pair of dark (3.8 cd/m^2) abutting contours (the same width as the white contours); the background luminance was then set to be the average luminance (see Fig. 4 for a schematic drawing). If orientation aftereffects from rapid adaptation were mainly due to the low-spatial-frequency components present in the hourglass contours, this high-pass-filtered version of the hourglass contours should produce much reduced aftereffects.

4. Experiment 1B

4.1. Can adapt-test compatibility or low-spatial-frequency components explain why brief adaptation produces strong contour-orientation aftereffects but much reduced texture-orientation aftereffects?

Observers SS and YS were tested in five brief adaptation (27 ms) conditions. The adaptors used were the X-patterned textures, the hourglass figure (as in Experiment 1A), and the high-pass-filtered version of the hourglass figure. The test stimuli used were the outline squares (as in Experiment 1A) and the grating-defined squares described above. There were five combinations

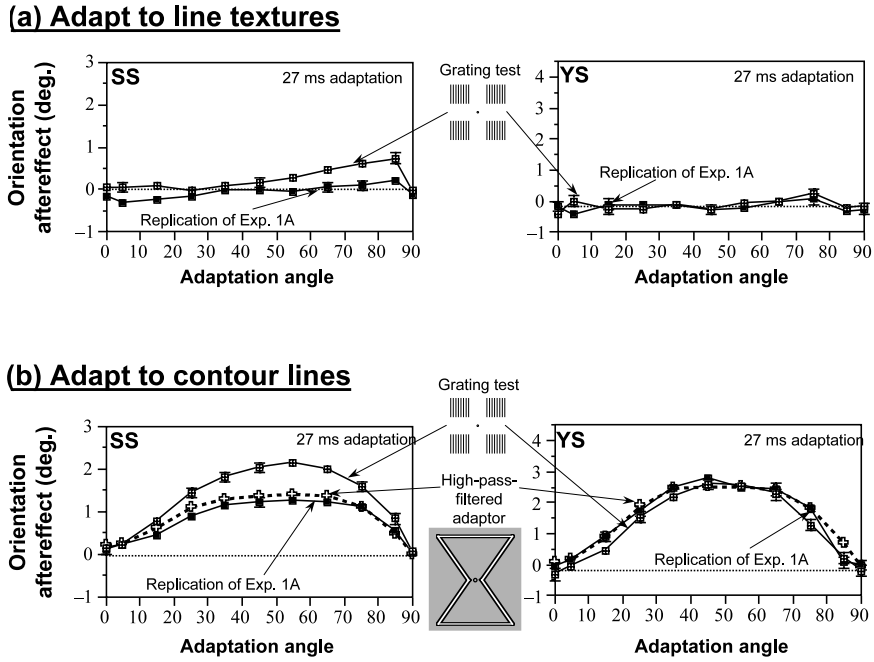

Fig. 4. The dependence of the orientation aftereffects on the adaptation angle—the control conditions with brief, 27 ms, adaptation (observers SS and YS; Experiment 1B). (a) The aftereffects from adaptation to the X-patterned line textures probed by the outline test squares (solid symbols; replication of Experiment 1A) and probed by the grating-defined test squares (crossed square symbols; see schematic drawing). (b) The aftereffects from adaptation to the hourglass contours probed by the outline test squares (solid symbols; replication of Experiment 1A) and probed by the grating-defined test squares (crossed square symbols). The open cross symbols indicate the aftereffects from adaptation to the high-pass-filtered hourglass figure (see schematic drawing) probed by the outline test squares.

of adaptors and test stimuli: (1) adapt to X-patterned textures and test with outline squares, (2) adapt to X-patterned textures and test with grating-defined squares, (3) adapt to hourglass figure and test with outline squares, (4) adapt to hourglass figure and test with grating-defined squares, and (5) adapt to high-pass-filtered hourglass figure and test with outline squares. The combinations (1) and (3) were identical to those tested in Experiment 1A. These reference conditions were re-tested so that they were measured in close temporal proximity to the new conditions.

For each adapt-test combination, orientation aftereffects were measured for all adaptation angles in one sitting. The double-staircase method was used; a 2-min break was inserted between successive measurements of the aftereffect as the adaptation angle was changed. At least a 1-h break (typically a 1-day break) was given before testing a new adapt-test combination. The five adapt-test combinations were tested once as the adaptation angle was varied from 0° through 90° in each session, and tested again as the adaptation angle was varied from 90° through 0° in each session. The observer YS went through this ten-session sequence once and SS went through it twice. The data (means and SEMs of staircase reversal values) were averaged across multiple measurements because the pattern of data remained unchanged across sessions.

4.2. Results and discussion

In Fig. 4, the filled square symbols indicate the replication conditions. For both observers, brief adaptation to the X-patterned textures produced virtually no aftereffects on the outline test squares (filled symbols in Fig. 4a). In contrast, brief adaptation to the hourglass contours produced broadly tuned aftereffects (filled symbols in Fig. 4b). The results from Experiment 1A were thus replicated.

According to the adapt-test compatibility hypothesis, the use of the grating-defined test squares should have reversed this pattern of results, yielding strong aftereffects for the X-patterned textures and much reduced aftereffects for the hourglass contours. This was not supported. The grating-defined test squares either made no difference (YS) or elevated the aftereffects for both adaptors (SS)—compare crossed square symbols with filled square symbols in Fig. 4a and b. According to the low-spatial-frequency hypothesis, the use of the high-pass-filtered version of the hourglass contours should have considerably reduced the aftereffects. This was not supported. The high-pass-

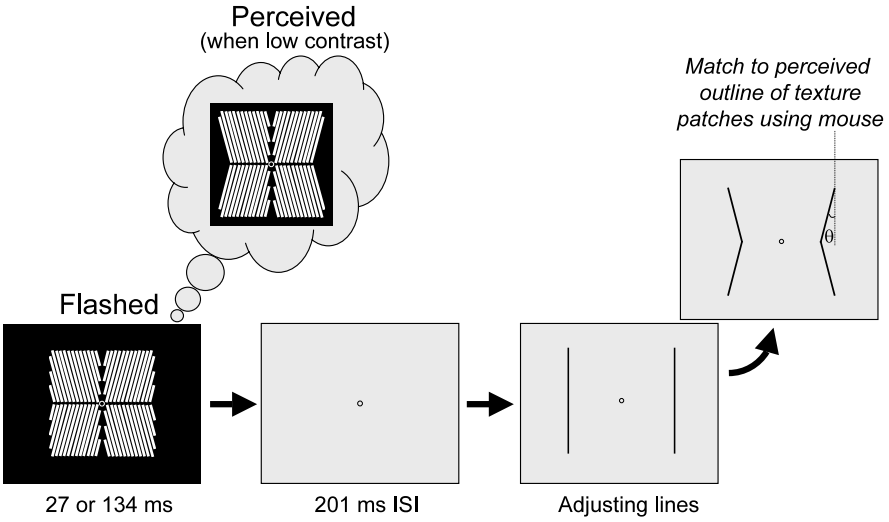

Fig. 5. Sequence of events in an experimental trial used to measure the perceived overall concavity/convexity of the briefly flashed X-patterned line textures (Experiment 2). The adjusting lines were initially straight, being aligned with the left and the right borders of the texture patches. Observers moved the computer mouse to vary the concavity/convexity of the adjusting lines until they matched the perceived degree of concavity/convexity, then clicked the mouse. Concavity was measured as a positive angle relative to vertical, $+\theta$, whereas convexity was measured as a negative angle, $-\theta$.

filtered hourglass contours (open cross symbols in Fig. 4b) produced aftereffects that were just as strong as those produced by the original (non-high-pass-filtered) hourglass contours (filled square symbols in Fig. 4b).

Thus, neither the adapt-test mismatch of spatial frequency contents nor the low-spatial-frequency components of the hourglass contours accounted for the fact that brief adaptation to the oriented contour lines produced strong aftereffects whereas brief adaptation to the oriented line textures produced much reduced or no aftereffects.

To further compare brief adaptation to contour-line orientation with brief adaptation to line-texture orientation, the contrasts of the adaptors were systematically varied in the next experiment. There were two specific aims. First, it was found in Experiment 1A that orientation aftereffects due to the hourglass contours saturated rapidly in time (27 and 2684 ms adaptation produced equivalent amounts of aftereffects; Fig. 3b). This experiment evaluated whether the contour-orientation aftereffect saturated rapidly with respect to adaptation duration, adaptation contrast, or contrast energy (contrast $\times$ exposure duration). If adaptation of the presumed contour-orientation mechanism depended on contrast energy, for example, doubling the adaptation duration should make the aftereffect saturate at half the contrast.

Second, an informal observation indicated that the X-patterned textures appeared to assume an overall concave shape (Fig. 5) when they were briefly presented and their contrast was low. The perception of these faint contours is probably due to a combination of eccentricity-dependent reduction in visual sensitivity (e.g. Rijsdijk, Kroon, & van der Wildt, 1978) and some interactions among local oriented receptive fields.[4] Regardless of the exact underlying cause of the faint contours, this phenomenon provided a critical test for the hypothesis that brief stimuli, whether hourglass or X-patterned textures, selectively adapt a contour-orientation mechanism which is different from the mechanism that produces line-texture orientation aftereffects with prolonged adaptation. If briefly presented contour lines and line textures both adapted the same orientation coding mechanism, but the line textures somehow adapted the mechanism weakly even at high contrast, then further weakening the line-texture adaptor by reducing its contrast should only weaken its already negligible orientation aftereffects. This predicts that briefly presented X-patterned textures should produce little orientation aftereffects at any contrast. Alternatively, if a rapidly adapting orientation coding mechanism existed and it selectively processed outline contour orientations (regardless of whether the hourglass or the X-patterned textures were presented), the X-patterned

[4] Many studies have demonstrated local facilitative interactions among co-oriented receptive fields along a smooth (co-axial) path, using Gabor patches that are variously aligned along different paths (e.g. Field, Hayes, & Hess, 1993; Bonneh & Sagi, 1998; Polat & Sagi, 1993; Polat & Norcia, 1996; Kapadia, Ito, Gilbert, & Westheimer, 1995). When the X-patterned line textures are low contrast and briefly flashed, visibility of the eccentric portions of lines that originate near the fixation point might be enhanced due to the collinearity-based facilitation cascading from ends near the fixation point (where visual sensitivity is high); lines that originate farther away from the fixation point (lines near the left and right ends of the texture patches) should not benefit from such facilitation. Diminishing these latter lines would result in concave contours (Fig. 5).

textures should not produce orientation aftereffects at high contrast because their outline contours are vertical and horizontal, but they should produce orientation aftereffects at low contrast when they appear to have faint concave outline contours.

5. Experiment 2

5.1. How do the contour-line and the line-texture aftereffects induced by brief adaptation depend on the contrast energy of adaptors?

The luminance of the adaptor lines was systematically varied from 3.8 cd/m^2 through 112 cd/m^2 against a dark background (3.8 cd/m^2); this was done by varying the value of the green gun from zero through maximum (CIE[.305,.570]; the red and blue guns being turned off) except for the highest luminance which was generated by setting all three color guns at maximum (CIE[.286,.301]). As a result, the contrast of the lines varied from 0.00 through 0.94. As before, the test stimulus was always high-contrast (-0.94, dark against a light background), and brief (27 ms), followed immediately by the random-dot mask (403 ms).

The adaptors used were the X-patterned textures and the hourglass figure. The adaptation angles were 75° for the line textures (optimum as seen in Fig. 3a) and 55° for the hourglass figure (roughly the middle of the broad tuning; see Fig. 3b and Fig. 4b). Two brief adaptation durations, 27 and 134 ms, were tested so that any contrast dependence obtained could be assessed as to whether it was due to dependence on contrast per se or on contrast energy. There were thus four adaptation conditions, 27 and 134 ms adaptation to the X-patterned textures, and 27 and 134 ms adaptation to the hourglass contours. The entire range of contrast was swept (from lowest to highest)[5] for these four adaptation conditions in separate sessions.

Three different perceptual phenomena were measured concurrently as a function of adaptation contrast, (1) visibility of the adaptors, (2) magnitude of the orientation aftereffects, and (3) perceived concavity (or convexity) of the outer edges of the X-patterned-texture adaptor. These measurements were made to determine how the orientation aftereffects saturated relative to the detection threshold of the adaptor, and whether brief adaptation to the X-patterned textures produced orientation aftereffects when they appeared to have faint concave outlines. For each adaptation contrast, the detection performance on the adaptor was measured first, using a two-interval-forced-choice (2IFC) method (unless the detection rate was 100% for the previous contrast value). To make the condition of these detection trials as similar as possible to the aftereffect trials, each detection trial consisted of two aftereffect trials presented back to back (with 1900 ms fixation screen in between). Only one of the intervals contained the adaptor. The observer's task was to indicate the interval in which the adaptor was presented; percent correct was computed based on 20 trials. Following a 2-min break, the orientation aftereffect was measured using the double-staircase method. Following another 2-min break, when the X-patterned textures were visible (i.e. 100% correct in the detection task), observers judged the perceived concavity (or convexity) of the outer contours using an adjustment technique. A flash of the X-patterned textures was followed (after the standard 201 ms ISI) by an adjustment display consisting of a fixation point and two vertical lines marking the left and the right vertical borders of the texture patches (Fig. 5). By moving the computer mouse, observers could bend these lines at the middle to match the perceived concavity (or convexity); the degree of perceived concavity was measured as the angle of the adjusted lines relative to vertical (θ indicated in Fig. 5). These three measurements were then repeated for a new contrast value following a 2-min break.

The three observers, SS, YS, and ET, were tested in all of the four adaptation conditions (at least a 1-h break, typically a 1-day break, was given between different conditions). Observers SS and YS were tested in these conditions previously (without the shape-matching task on the X-patterned textures); the new data (presented here) replicated the previous results unless otherwise noted.

5.2. Results and discussion

For the hourglass contours, the aftereffects (Fig. 6, filled symbols in middle panels) began to rise above zero when the contours became reliably visible (i.e. when 2IFC detection performance just reached 100%; see filled symbols in top panels) whether the adaptation duration was 27 (Fig. 6a) or 134 ms (Fig. 6b). The aftereffects thus depended on the visibility rather than the contrast per se of the adaptor. This point is more clearly illustrated in Fig. 7. The aftereffects from 27 and 134 ms adaptation to the hourglass contours are plotted together (along with the detection data) as a function of contrast energy (contrast $\times$ exposure duration). The alignment of the curves indicates that the aftereffects depended primarily on contrast energy (rather than contrast or exposure duration per se). The aftereffects saturated within about a factor-of-three increase in the contrast energy relative to that required for reliable detection of the adaptors.

As shown in Fig. 6, the X-patterned textures also produced orientation aftereffects when they became just reliably visible (open symbols in the top and middle

[5] The luminance was always varied from lowest to highest in order to minimize carry-over adaptation effects from measurement to measurement.

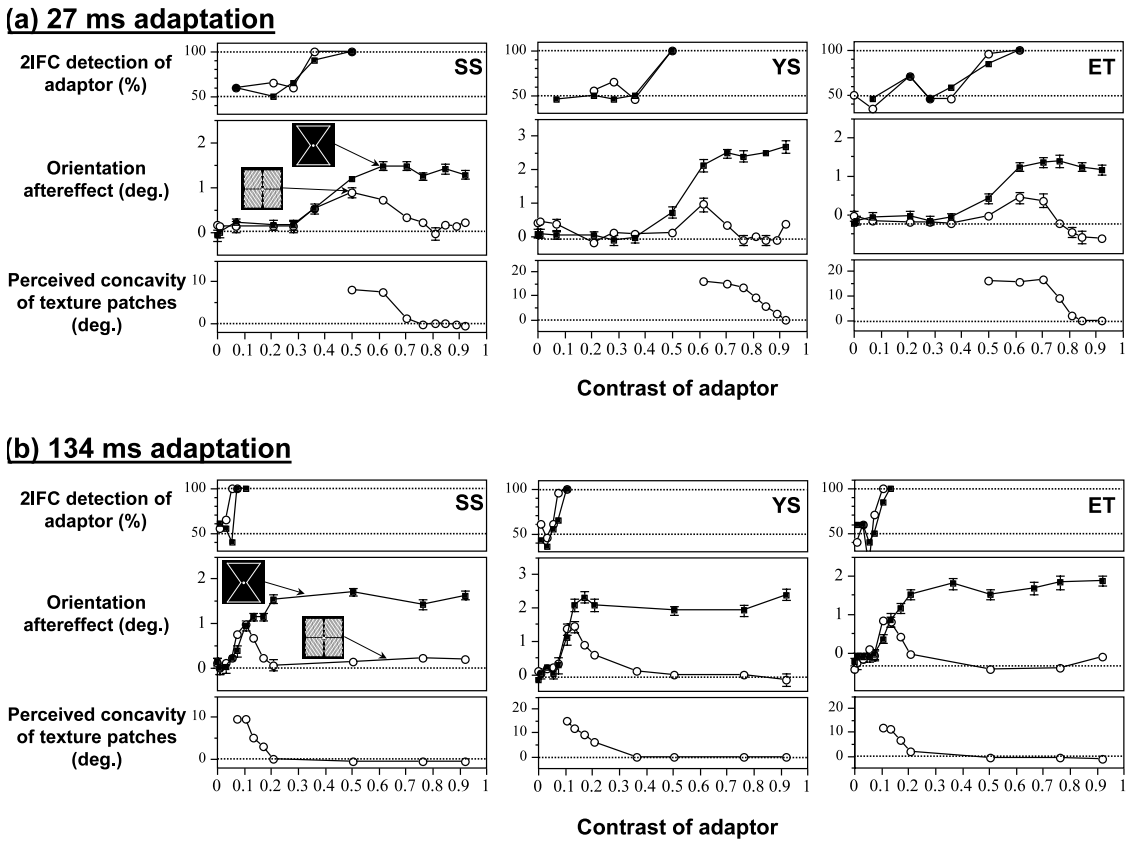

Fig. 6. The dependence of (1) the visibility of the adaptors, (2) the orientation aftereffects, and (3) the perceived overall concavity of the X-patterned-texture adaptor, on the contrast of the adaptors (observers SS, YS, and ET; Experiment 2). (a) 27 ms adaptation and (b) 134 ms adaptation to the X-patterned line textures (open symbols) and to the hourglass contours (filled symbols). Top panels—2IFC detection performances on the adaptors. Middle panels—the orientation aftereffects. Bottom panels—the perceived overall concavity of the texture patches (θ described in Fig. 5).

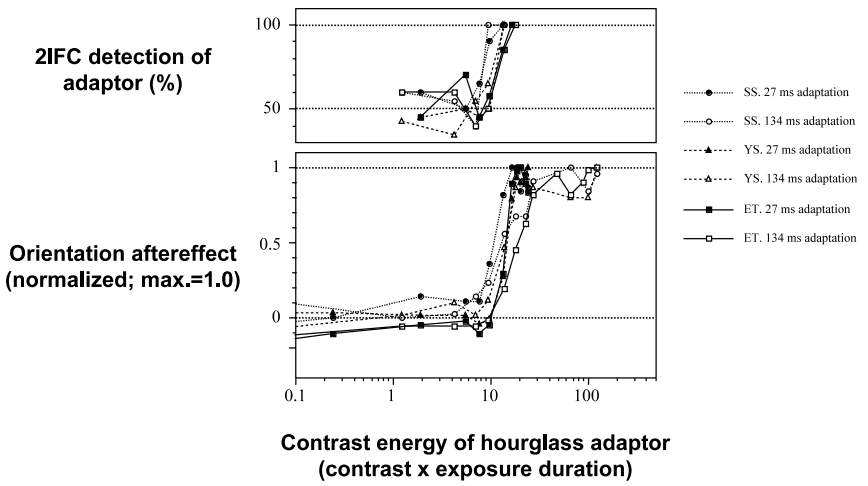

Fig. 7. The data for the hourglass adaptors from Fig. 6 have been re-plotted to show that the 2IFC detection of the adaptors (top panel) and the orientation aftereffects (bottom panel) both depended on contrast energy (contrast × exposure duration). The 27 and 134 ms adaptation data from SS, YS, and ET are shown together. The data for the aftereffects have been normalized such that the maximum is 1 under each condition for each observer.

panels). However, the aftereffects occurred only for a limited range of low contrast. Consistent with the pilot observation, the texture patches appeared to have concave outline contours when they became just reliably visible (bottom panels); as the contrast was further increased, the outline appeared less concave and eventually appeared vertical at high contrast. Furthermore, the decline in the line-texture-induced aftereffects with increasing contrast appears to have closely followed the decline in the perceived concavity of the texture patches[6] (compare open symbols in middle and bottom panels). If this co-variation implied a causal relationship, it would be consistent with the idea that faint outline contours generated by the visual field inhomogeneity engaged the rapidly adapting contour orientation mechanism.

As discussed above, this finding provides evidence in support of the idea that brief stimuli (27 ms and at least up to 134 ms) selectively adapt a contour-orientation mechanism (regardless of whether the hourglass contours or the X-patterned textures are presented), and against the idea that a single orientation coding mechanism is more optimally adapted by contour-line stimuli than by line-texture stimuli under brief presentation. The presumed contour-orientation mechanism can be adapted whether contours are defined by bright lines, high-pass-filtered lines, or faint outline contours generated by spatial inhomogeneity of visual sensitivity. Adaptation of this mechanism depends on the visibility of the adaptor and saturates at low contrast energy (within about three times the value that is required for the image to be reliably visible). In the next experiment, overlapping contours were used to assess how this rapidly adapting contour orientation mechanism might be modulated by selective attention.

Recently, Spivey and Spirn (2000) reported that tilt aftereffects produced by prolonged adaptation (60 s) to oriented gratings (line textures) could be modulated by selective attention during adaptation. A left tilted grating consisting of green bars and a right tilted grating consisting of red bars (square wave, 0.5 cyc/deg, tilted $\pm 15°$ relative to vertical) were superimposed within a circular aperture during adaptation; observers were instructed to attend to one or the other grating while fixating the central fixation point. Following adaptation, the observers indicated whether a vertically oriented test grating appeared tilted to left or right. Spivey and Spirn found that the vertical test grating appeared tilted away from the previously attended grating 28% more frequently (on average) than it appeared tilted away from the previously ignored grating. Though this effect of attentional modulation was statistically significant, it was a small effect in that in many of the trials, their observers did not see the vertical test grating tilted away from the previously attended grating.

The current experiment explored the possibility that the rapidly adapting contour-orientation mechanism might be more susceptible to attentional modulation than the texture-orientation mechanism. Furthermore, to determine whether the effectiveness of selective attention depended on the salience of the attended pattern (relative to the ignored pattern), the contrast of one of the overlapping patterns was systematically varied while the contrast of the other pattern was fixed; observers attended to either of the two overlapping patterns.

6. Experiment 3A

6.1. How does selective attention modulate the rapidly adapting contour-orientation aftereffects?

The experimental conditions were similar to those used in Experiment 2 except that the diamond contours were superimposed on the hourglass contours (see schematic drawings in Fig. 8). While the contrast of the diamond was fixed at a high value (0.75; 26.5 cd/m^2 against 3.8 cd/m^2; CIE[.601,.352]; red gun at maximum value), the contrast of the hourglass was varied from 0.00 (3.8 cd/m^2) through 0.94 (112 cd/m^2) as in Experiment 2. The two shapes were colored differently (red for the diamond, and green to white—highest contrast only—for the hourglass) to facilitate selective attention (e.g. Suzuki & Grabowecky, 2000). The observer attended to either the high-contrast diamond or the variable-contrast hourglass in the adaptation display. The test stimulus was again high contrast (-0.94, dark against a light background) and brief (27 ms), followed immediately by the random-dot mask (403 ms).

The duration of adaptation was 134 ms. The shortest duration, 27 ms, was not used because the colors appeared de-saturated. As found in Experiment 2, 134 ms adaptation was still short enough to selectively engage the contour-orientation mechanism; the line-texture stimuli produced virtually no aftereffects with 134 ms adaptation at high contrast (Fig. 6b). As in Experiment 2, the hourglass contours were oriented 55°; the diamond contours were oriented in a complementary manner.

There were a total of three adaptation conditions: (1)

[6] Note that perceived concavity of the texture patches decayed appreciably slower than the orientation aftereffect for observer YS following 27 ms adaptation. YS had some difficulty reproducing the perceived outline contours of the low-contrast texture patches under 27 ms presentation (no difficulty under 134 ms presentation). Furthermore, when YS was tested in the same experiment previously (without the part of judging concavity of outline contours), 27 ms adaptation to the texture patches produced no aftereffect at any contrast; in all other respects, her current data replicated her previous data. It might be that the faint concave contours were not spontaneously salient to YS under 27 ms presentation in the previous testing. The concurrent contour judgment task here might have made her notice (pay attention to) these faint contours. Indeed, as demonstrated in Experiments 3A and 3B, selective attention strongly modulated the contour-based orientation aftereffects under brief adaptation.

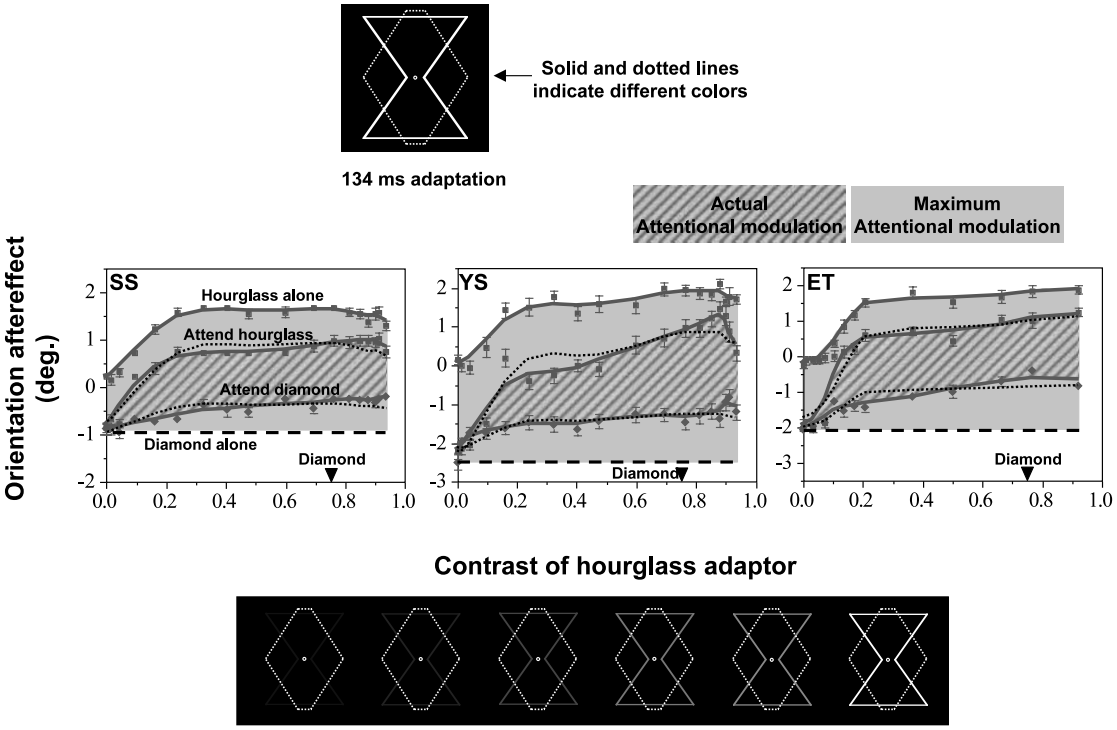

Fig. 8. Attentional modulation of the orientation aftereffect for the overlapping hourglass and diamond figures; the contrast of the hourglass figure was varied while the diamond figure had a fixed contrast of 0.75 (observers SS, YS, and ET; Experiment 3A). Note that the height of the diamond figure was slightly extended so that the two figures did not overlap completely at the top and bottom. The hourglass and the diamond figures had different colors (represented by the solid and dotted lines). Adaptation duration was 134 ms. In each graph, the top curve shows the aftereffect from adaptation to the hourglass figure alone, the middle curve shows the aftereffect from attending to the hourglass figure in the overlapping stimulus, the bottom curve shows the aftereffect from attending to the diamond figure in the overlapping stimulus, and the dashed line shows the aftereffect from adaptation to the diamond figure alone. For all graphs, the upper bound of the potential attentional modulation is indicated by the gray region and the actual attentional modulation is indicated by the hatched region. The data have been smoothed using a five-channel binomial fit. The "attend hourglass" and "attend diamond" curves are fit by a simple model of selective attention (dotted curves), which assumes that the effectiveness of selective attention is independent of the relative contrast of the attended and the ignored figures (see text for details).

attend to the hourglass contours presented alone, (2) attend to the hourglass contours while ignoring the diamond contours in the overlapping pattern, and (3) attend to the diamond contours while ignoring the hourglass contours in the overlapping pattern. For each adaptation condition, the aftereffects were measured in the order of low to high contrast of the hourglass in one session, using the double-staircase method. As in Experiment 2, a 2-min break was inserted between successive measurements of the aftereffect as the contrast of the hourglass contours was stepped up. At least a 1-day break was given between conditions.

Each condition was run once for observer SS and ET. The selective attention conditions were tested three times for observer YS due to increased variability; the data presented for YS are the means of these three runs; the error bars are also averaged across these runs.

6.2. Results and discussion

In Fig. 8, the positive Y values indicate the aftereffects in the convex direction and the negative Y values indicate the aftereffects in the concave direction. In each graph, the top curve represents the condition in which the hourglass contours were presented alone during adaptation. This curve establishes the upper bound for the effect of selectively attending to the hourglass contours which tend to produce convex aftereffects. The bottom curve represents the aftereffect when the observer attended to the diamond contours. Its left-most value corresponds to 0.00 contrast of the hourglass, that is, the diamond being presented alone; the dashed line thus indicates the upper bound for the effect of selectively attending to the diamond contours which tend to produce concave aftereffects. The gray region (bound by the top curve and the dashed line) therefore indicates the maximum possible attentional modulation of the aftereffect; if attentional selection of the hourglass contours were perfect, the aftereffect would be the same as when the hourglass contours were presented alone (the top curve); if attentional selection of the diamond contours were perfect, the aftereffect would be the same as when the diamond contours were presented alone (the dashed line).

The hatched region bound by the middle curve (attending to the hourglass contours) and the bottom curve

(attending to the diamond contours) represents the actual attentional modulation; this region indicates the difference in the aftereffect between attending to the hourglass contours and attending to the diamond contours. As seen in Fig. 8, attentional modulation of the aftereffect was substantial for all three observers. Notably, selective attention was effective in modulating the aftereffect even when the attended figure (hourglass) was much lower-contrast than the ignored figure (diamond) so long as the attended hourglass contours had sufficient contrast energy to produce reliable aftereffects without the overlapping diamond contours. In fact, it appears that the effect of selective attention remained relatively constant while the relative contrast of the hourglass and the diamond was widely varied. To evaluate this more quantitatively, the data were fit using a simple linear model of attentional modulation.

Aftereffects under the selective attention conditions were assumed to be predicted by linear combinations of aftereffects when the individual adaptors (which produced opponent aftereffects) were tested alone; that is, AE(attend-hourglass, C) or AE(attend-diamond, C) $= w_{\text{hourglass}} \cdot \text{AE}(\text{hourglass alone}, C) + w_{\text{diamond}} \cdot \text{AE}(\text{diamond alone}, C)$, where AE abbreviates aftereffect, which is a function of the adaptation condition and C (the relative contrast of the hourglass and the diamond), and $w_{\text{hourglass}}$ and w_{diamond} are linear attention weights; $w_{\text{hourglass}}$ should be larger than w_{diamond} when the hourglass is attended and vice versa. The key feature of the model was that the two attention weights, the fitting parameters, were assumed to be independent of C. The fitting was done on the basis of the smoothed versions of the data (continuous curves shown in Fig. 8), using a least-squares fitting algorithm (Mathematica, Wolfram Research, Inc.). The fits[7] (shown as dotted curves in Fig. 8) are reasonably good, suggesting that selective attention modulated adaptation of the orientation coding units underlying the aftereffect in a largely contrast invariant manner. However, this post hoc inference requires confirmation in a future study in which alternative models are tested.

The characteristics of the rapidly adapting contour-orientation aftereffects obtained so far, (1) broad orientation tuning, (2) rapid saturation with contrast energy, (3) relative independence with respect to how the contours are defined, and (4) strong attentional modulation, suggest that these aftereffects may be due to adaptation of a high-level visual form processing mechanism (the relevant neurophysiology literature is reviewed in the general discussion). In the final experiment, the size of the adaptor was varied systematically while the size of the test stimulus was kept constant. Attentional modulation of the aftereffect was also examined. If the contour-orientation aftereffects demonstrated so far were due to the sum of local orientation aftereffects, they should diminish substantially as the size of the adaptor was reduced so that it did not overlap at all with the four test squares (see the left most adaptor shown in Fig. 9). In contrast, if the aftereffects were due to adaptation of a high-level shape-coding mechanism (e.g. coding of overall convexity), the aftereffects might be relatively scale tolerant because high-level neurons that are tuned to global shapes exhibit various degrees of scale invariance (e.g. Tanaka, 1996; Ito, Tamura, Fujita, & Tanaka, 1995; Hikosaka, 1999). This experiment also examined how the effectiveness of attentional selection depended on the scale of the overlapping stimuli.

7. Experiment 3B

7.1. How do rapidly adapting contour-orientation aftereffects and their attentional modulation depend on the size of adaptors?

The adaptors were the red diamond contours superimposed on the green hourglass contours as in Experiment 3A. The red and green contours both had 75% contrast (26.5 cd/m^2 against 3.8 cd/m^2); as shown in Fig. 8, this contrast yielded strong attentional modulation in Experiment 3A. The vertical extent of the adaptor was varied from 15.8° to 2.3° (see Fig. 9 for schematic drawings). Since the gaps between the squares in the test stimulus subtended 3.39° (Fig. 1), the smallest adaptor was completely within the central gap region of the test stimulus (no overlap with the test squares).

There were four adaptation conditions: (1) attend to the hourglass contours presented alone, (2) attend to the hourglass contours while ignoring the diamond contours in the overlapping pattern, (3) attend to the diamond contours while ignoring the hourglass contours in the overlapping pattern, and (4) attend to the diamond contours presented alone. For each adaptation condition, the aftereffects were first measured in the order of largest to smallest adaptor in one session. The double-staircase method was used and a 2-min break was given before moving on to a new size. At least a 1-h break (typically a 1-day break) was given between adaptation conditions. The entire set of four adaptation conditions was tested again while the size of the adaptor was varied from smallest to largest in each session. The data were averaged across the two runs for each condition. All three observers, SS, YS, and ET, participated.

[7] The attention weights obtained are as follows. Here, w_{h} indicates $w_{\text{hourglass}}$ and w_{d} indicates w_{diamond}. For SS, $w_{\text{h}} = 1.15$ and $w_{\text{d}} = 1.07$ when the hourglass was attended, whereas $w_{\text{h}} = 0.42$ and $w_{\text{d}} = 1.15$ when the diamond was attended. For YS, $w_{\text{h}} = 1.69$ and $w_{\text{d}} = 1.02$ when the hourglass was attended, whereas $w_{\text{h}} = 0.48$ and $w_{\text{d}} = 0.93$ when the diamond was attended. For ET, $w_{\text{h}} = 1.39$ and $w_{\text{d}} = 0.74$ when the hourglass was attended, whereas $w_{\text{h}} = 0.57$ and $w_{\text{d}} = 0.93$ when the diamond was attended.

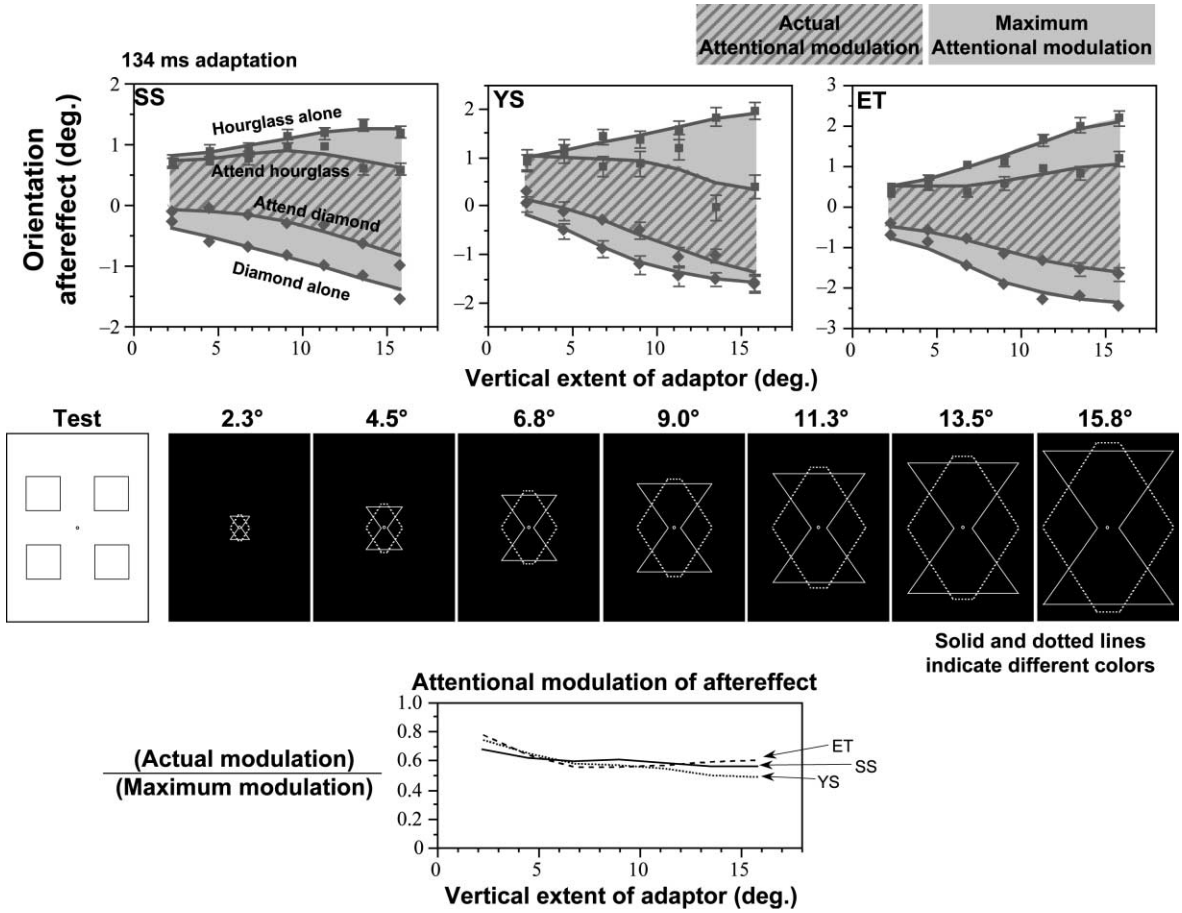

Fig. 9. Scale dependence of the orientation aftereffect and its attentional modulation for the overlapping hourglass and diamond figures (observers, SS, YS, and ET; Experiment 3B). The magnitudes of the orientation aftereffects are plotted as a function of the vertical extent of the adaptors. As in Experiment 3A, the hourglass and the diamond figures had different colors (represented by the solid and dotted lines). Adaptation duration was 134 ms. In each graph, the top curve shows the aftereffect from adaptation to the hourglass figure alone, the upper middle curve shows the aftereffect from attending to the hourglass figure in the overlapping stimulus, the lower middle curve shows the aftereffect from attending to the diamond figure in the overlapping stimulus, and the bottom curve shows the aftereffect from adaptation to the diamond figure alone. For each observer, the upper bound of the potential attentional modulation is indicated by the gray region and the actual attentional modulation is indicated by the hatched region. The data have been smoothed using a five-channel binomial fit (solid curves). The bottom panel shows the degree of attentional modulation, [actual modulation]/[maximum modulation] = [{attend-hourglass condition} − {attend-diamond condition}]/[{hourglass-alone condition} − {diamond-alone condition}], as a function of the vertical extent of the adaptors (computed based on the smoothed data).

7.2. Results and discussion

In Fig. 9, the top and bottom curves indicate the perceived convexity (positive values) and concavity (negative values) of the test stimulus when the hourglass contours were presented alone (top curves) and when the diamond contours were presented alone (bottom curves) during the 134 ms adaptation period. Though the magnitude of the aftereffect gradually decreased as the adaptor was made smaller, it persisted even for the smallest adaptor which did not overlap with the test stimulus. Therefore, it is difficult to explain the aftereffects induced by the hourglass and the diamond contours solely in terms of a sum of local orientation interactions.

The two middle curves show the aftereffects obtained when observers attended to the hourglass contours (upper middle curve) and the diamond contours (lower middle curve) while the two types of contours were superimposed during adaptation. As in Experiment 3A, the gray regions in Fig. 9 represent the maximum possible attentional modulation of the orientation aftereffect while the hatched regions indicate the actual levels of attentional modulation. For all three observers, attentional modulation was again substantial and remained relatively constant, 50% to 60% relative to perfect, across all sizes of the adaptor tested (bottom panel). In particular, the fact that reliable attentional modulation was obtained for the smallest adaptor indicates that the spatial resolution of attention in selecting contours for the orientation aftereffect was at least about 0.6° (the maximum distance between the overlapping hourglass and diamond contours for the 2.3° adaptor).

8. General discussion

8.1. Resolving discrepancies with previous results

8.1.1. Previous results demonstrated reliable tilt aftereffects following brief adaptation to a line texture stimulus

As mentioned earlier, Sekuler and Littlejohn (1974) obtained reliable tilt aftereffects following adaptation to a briefly flashed line texture stimulus (a square-wave grating; 4 cyc/deg; contrast = 0.91; slanted $\pm 10°$ from horizontal). Following a brief test period (100 ms), their observers adjusted the orientation of a bright test bar (contrast = 0.38) to apparent horizontal. The adaptor and the test stimulus were repeated until the observers were satisfied with their adjustments. They obtained reliable tilt aftereffects when the adaptation duration was as short as 18 ms, and suggested that adaptation saturated around 18 ms. Though Greenlee and Magnussen (1987) subsequently reported that tilt aftereffects increased logarithmically through an hour of adaptation, Sekuler and Littlejohn's result apparently contradicts the current finding that the line textures produced little aftereffect when presented briefly (27 ms).

There are several factors that may explain this discrepancy. First, since their observers adjusted the test line to apparent horizontal, non-visual factors such as gravity may have influenced their aftereffect (e.g. Wolfe & Held, 1982). As mentioned earlier, the present study attempted to isolate the visual component of orientation aftereffects using a shape-distortion paradigm.

Second, Sekuler and Littlejohn presented their test stimulus immediately following the adaptor, whereas a 201 ms blank ISI was inserted between adaptation and test in this study. If this difference in ISI is critical, brief (27 ms) adaptation to the line-texture stimulus used in the current study should also produce reliable orientation aftereffects if the ISI between adaptation and test was made very short. This possibility was tested. The ISI was varied from 0 ms through 215 ms; the aftereffect was measured for the X-patterned line textures (112 cd/m^2) using the double-staircase method. The measurements were made once in the ascending order of the ISI and once in the descending order of the ISI. As before, at least a 2-min break was inserted between successive measurements of the aftereffect as the ISI was varied. The average data are shown for observers SS and YS in Fig. 10. Indeed, reliable aftereffects were obtained for very short ISIs. Thus, it is possible that brief adaptation to line textures produces a rapidly decaying orientation aftereffect (lasting about 50 ms). However, it is also possible that this extremely short-lasting aftereffect is actually a tilt illusion effect (e.g. O'Toole & Wenderoth, 1977; Magnussen & Kurtenbach, 1980; Wade, 1980) due to visible persistence (e.g. Turvey, 1978; Bowling & Lovegrove, 1980) of the adaptor.

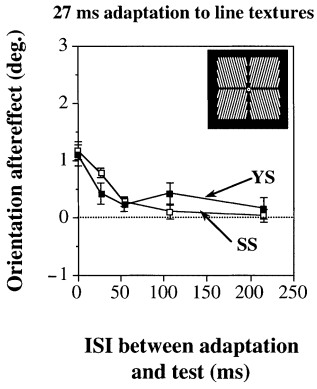

Fig. 10. The orientation aftereffect from 27 ms adaptation to the X-patterned line textures with very short inter-stimulus-intervals (ISI) between adaptation and test.

8.1.2. Previous studies found narrowly tuned tilt aftereffects following adaptation to a single bar or to a line bent in the middle

Previous studies using a single bar (a type of line contour stimulus; e.g. Magnussen & Kurtenbach, 1980; O'Shea et al., 1993) and a vertical line bent in the middle (e.g. Paradiso et al., 1989) as the adaptors and the test stimuli, obtained narrowly tuned angular functions of tilt aftereffects, whereas the current study found the aftereffects due to outline contours to be rather broadly tuned. Magnussen and Kurtenbach used prolonged adaptation (initial 2-min adaptation plus 10-s top-up adaptation preceding each trial) and fairly long test (1.5 s) during which their observers adjusted the orientation of a spatially displaced comparison line to match the perceived orientation of the test line. O'Shea et al. used briefer adaptation (1 s) followed by a 100 ms ISI and a brief test (100 ms, no mask); the aftereffect was measured by determining the degree of tilt of the test line required to cancel the aftereffect, using a staircase method. Paradiso et al. also used brief adaptation (1.5 s) followed by a 100 ms ISI and a brief test (50 ms, no mask); the aftereffect was also measured by a cancellation technique, but using a method of constant stimuli. The current study and the studies by O'Shea et al. and Paradiso et al. thus used a similar range of adaptation duration and a similar technique for measuring orientation aftereffects. It is possible that relatively minor differences in ISI (201 versus 100 ms) and test duration (27 ms with backward masking versus 100 or 50 ms with no masking) contributed to the differences in angular tuning.

Alternatively, it might be the case that orientation is coded differently when oriented contours are presented as components of a simple global figure (as in the current study) as opposed to when a single oriented line (O'Shea et al., 1993) or a line bent in the middle (Paradiso et al., 1989) is presented. As mentioned above, tilt aftereffects induced by a single line may be affected by non-visual

factors such as gravity. Note that the "<" shaped contours used by Paradiso et al. can be considered a half of the hourglass (or the diamond) figure used in the current study. The orientation aftereffects examined here might be due to adaptation of a high-level shape coding mechanism tuned to global configurations of oriented contours (e.g. convexity and concavity) as discussed below. A half of the hourglass figure might not be sufficient to engage this global mechanism.

8.2. Implications of the current results

While numerous previous studies examined representations of orientation defined by various surface features (e.g. luminance, color, subjective contours, binocular disparity, texture, and motion), this study examined representations of orientation with regard to two distinct roles that orientation plays, contour orientation and texture orientation. The study was initially motivated by a hypothesis that the visual system might code orientation of outline contours rapidly, and separately from orientation of line textures. Specifically, it was hypothesized that brief exposure might selectively adapt coding of contour orientation, producing strong contour-orientation aftereffects, without affecting coding of line texture orientation, producing negligible texture-orientation aftereffects. A shape-distortion paradigm and brief tests (27 ms, backward masked) were used.

Adaptation to the line texture stimuli produced narrowly tuned orientation aftereffects (strongest for adaptation angle at about $\pm 15°$ from the test orientation, comparable to typically reported tilt aftereffects) following relatively long adaptation (2684 ms), but produced much reduced (or no) aftereffects following brief adaptation (27 and 134 ms). In contrast, adaptation to the contour line stimuli produced broadly tuned orientation aftereffects (strongest for adaptation angle at about $\pm 30°$ to $\pm 50°$ from the test orientation) whether adaptation was long (2684 ms) or brief (27 and 134 ms) (Experiment 1A). Potential explanations of this dissociation based on the spatial frequency contents of the adaptors and the test stimulus were ruled out in Experiments 1B and 2. The hypothesis that both contour-line and line-texture stimuli adapted a common orientation-coding mechanism, but briefly presented line-texture adaptors were somehow suboptimal, was ruled out in Experiment 2.

The overall results thus support the initial hypothesis that briefly exposed stimuli selectively adapt a mechanism that rapidly encodes contour orientation. Furthermore, the parametric results suggest that this rapidly adapting contour-orientation mechanism may involve a high-level neural representation of global shapes. As discussed below, the psychophysical characteristics of the contour-orientation aftereffects with brief adaptation obtained in the current study appear to parallel the response characteristics of high-level visual neurons tuned to global shapes in the ventral visual pathway (V4 through IT, thought to be involved in visual form processing; e.g. Ungerleider & Mishkin, 1982; Mishkin, Ungerleider, & Macko, 1983; Tanaka, 1996; Logothetis & Sheinberg, 1996).

First, the contour orientation aftereffects were broadly tuned (Experiments 1A and 1B). Orientation tuning of cells (for grating stimuli) tends to become progressively broader from the lower visual areas to the higher visual areas; median orientation tuning bandwidths (full width at half height) increase from about 30° to 40° in V1 (e.g. Vogels & Orban, 1994; Geisler & Albrecht, 1997) to about 40° to 50° for the orientation selective cells in V4 (e.g. Desimone & Schein, 1987; McAdams & Maunsell, 1999), and to about 70° in IT (Vogels & Orban, 1994). For a rough comparison, the tuning of the line-texture orientation aftereffects (following 2684 ms adaptation) was about 20° to 30°, whereas the tuning of the contour orientation aftereffects was about 60° (Figs. 3 and 4).

Second, the contour orientation aftereffects were relatively indifferent as to how the contours were defined (bright contours, high-passed-filtered contours, or faint contours due to spatial inhomogeneity in visual sensitivity; Experiments 1B and 2). Though many IT cells tuned to global shapes show preferences for specific color, contrast polarity, and contour type (e.g. outline or solid shapes; luminance-, motion-, or texture-defined contours), some proportion of IT cells respond to their preferred shapes relatively independently of variations in image features that define those shapes (e.g. Komatsu, Ideura, Kaji, & Yamane, 1992; Sato, Kawamura, & Iwai, 1980—variations in color; Rolls & Baylis, 1986; Ito, Fujita, Tamura, & Tanaka, 1994—variations in contrast polarity; Ito et al., 1994; Sary et al., 1995—variations in contour type).

Third, the contour orientation aftereffects saturated at low contrast energy (within about a factor-of-three increase in contrast energy relative to the value that makes the adaptors just reliably visible; Experiment 2). The responses of cells in the higher visual areas tend to saturate at lower contrast than the responses of cells in V1 (e.g. Sclar, Maunsell, & Lennie, 1990—V1 versus MT; Cheng, Hasegawa, Saleem, & Tanaka, 1994—V1 versus MT and V4; responses of IT cells also seem to be largely luminance invariant; e.g. Gross, Rocha-Miranda, & Bender, 1972; Sato et al., 1980). Median half saturation contrasts (contrasts required to generate half of the maximum responses) are 0.32–0.33 in V1 (Sclar et al., 1990; Geisler & Albrecht, 1997), 0.30 in V4 (Cheng et al., 1994), 0.07–0.16 in MT (Sclar et al., 1990; Cheng et al., 1994), and ~ 0.20 in IT (face selective cells; Rolls & Baylis, 1986). For a rough comparison, the half saturation contrasts for the contour orientation aftereffect with 134 ms adaptation (stimuli used in the physiological studies were presented for longer than 100 ms) were

between 0.10 and 0.20 for the three observers (Fig. 6b). Furthermore, many cells in IT show rapid gain control (adaptation); a brief exposure (350–500 ms) to a first stimulus substantially reduces the cells' responses to a second stimulus (presented 300–2000 ms later), especially when the second stimulus is identical or similar to the first stimulus (e.g. Miller, Li, & Desimone, 1993; Lueschow, Miller, & Desimone, 1994; Vogels, Sary, & Orban, 1995; but these results depend on the recording location within IT, the variety of stimuli used, and individual variability among monkeys; Vogels & Orban, 1994).

Fourth, the contour orientation aftereffects were strongly modulated by selective attention (commonly 40% to 60% modulation; Experiments 3A and 3B). Electrophysiological and brain imaging research as well as neurophysiological research have shown that attentional modulations of neural responses are generally larger in the higher visual areas (e.g. V4 and IT) than in V1 (e.g. McAdams & Maunsell, 1999; Haenny & Schiller, 1988; Luck, Chelazzi, Hillyard, & Desimone, 1997; Heinze et al., 1994; Mangun, Hillyard, & Luck, 1993; Kastner, De Weerd, Desimone, & Ungerleider, 1998; but attentional selection in V1 can be quite sophisticated—e.g. stronger response to the attended contour than to an overlapping distractor contour; Roelfsema, Lamme, & Spekreijse, 1998). It is also known that attentional modulation is weak when only one stimulus is presented within a cell's receptive field (when a monkey attends to that stimulus or a stimulus outside the receptive field); average response modulation is 18% to 26% in V4 (Spitzer, Desimone, & Moran, 1988; McAdams & Maunsell, 1999) and only 8% in V1 (McAdams & Maunsell, 1999). Strong attentional modulation occurs when multiple stimuli exist within a cell's receptive field; when two stimuli are presented within a receptive field of a cell in V2, V4, or IT, the cell responds mainly on the basis of the attended stimulus while ignoring the unattended stimulus (e.g. Moran & Desimone, 1985; Reynolds, Chelazzi, & Desimone, 1999; Luck et al., 1997; Chelazzi, Duncan, Miller, & Desimone, 1998). In other words, attention substantially increases the contribution of the attended stimulus relative to the contribution of the ignored stimulus in determining a cell's response, with respective contributions of $\sim 70\%$ for an attended stimulus to $\sim 30\%$ for an ignored stimulus in V2, $\sim 80\%$ to $\sim 20\%$ in V4 (for cells that are significantly modulated by attention; Reynolds et al., 1999), and nearly 100% to 0% in IT (attentional modulation reaching maximum at about 200 ms following stimulus onset when the competing stimuli are both presented in the contralateral visual hemifield and the monkey makes a saccade to the attended target; Chelazzi et al., 1998). Since cells in the higher visual areas tend to have progressively larger receptive fields[8], it is more likely that competing stimuli fall within their individual receptive fields. Cells in the higher visual areas are thus particularly sensitive to attentional modulation.

Fifth, the contour orientation aftereffects were relatively scale tolerant (Experiment 3B). Ito et al. (1995) reported that 21% of the IT cells they tested exhibited rather broad size tuning (greater than four octaves) for their preferred shapes (also see Tanaka, 1996; Hikosaka, 1999—degree of size invariance being more pronounced in the anterior part of IT, TE, relative to the posterior part of IT, TEO).

Finally, the effectiveness of selective attention in modulating the contour-orientation aftereffects remained relatively constant across changes in the contrast and the scale of the attended stimuli (Experiments 3A and 3B). These results are consistent with the idea that attention modulated adaptation of high-level cells whose responses saturate at low contrast and are relatively scale invariant.

If the rapidly adapting contour-orientation aftereffects are indeed mediated by a high-level visual area in which cells are tuned to global shapes, it is possible that the contour-orientation aftereffects obtained here are in fact aftereffects of global configurations of oriented contours (such as convexity and concavity). If so, these aftereffects might belong to the class of global shape aftereffects reported recently. Suzuki and colleagues reported a series of shape aftereffects for basic geometric features (e.g. aspect ratio, taper, overall curvature, and skew; Suzuki & Cavanagh, 1998; Suzuki, 1999). These shape aftereffects have been shown to occur across large spatial gaps (up to 12° under appropriate conditions) when the adaptor and the test stimulus (backward masked) are presented briefly (e.g. 30 ms) in a rapid succession (e.g. ISI = 200 ms) as in the current paradigm. The considerable degree of position invariance and subsequently reported invariance for surface features (e.g. color-defined versus luminance-defined; Rivest et al., 1997) and relative tolerance for size changes (e.g. Rivest et al., 1998; also see Regan & Hamstra, 1992), suggest that these shape aftereffects are mediated by rapid adaptation of high-level visual neurons, presumably in IT, which are tuned to simple geometric shapes (e.g. Fujita, Tanaka, Ito, & Cheng, 1992; Tanaka, 1996). To support the involvement of the temporal cortex in at least one such shape aftereffect, a recent neuropsychological study found that the aspect-ratio aftereffect tended to disappear in patients with temporal lobe

[8] e.g. Foster et al., 1985—mean = 1.1° for V1 and 3.0° for V2 for parafoveal regions; Desimone and Schein, 1987—RFs in V4 are 4–7 times as large as those in V1 for parafoveal regions; Gross et al., 1972; Desimone and Gross, 1979; Ito et al., 1995—RFs in IT have median size of $\sim 30°$, but up to $\sim 100°$.

damage (Kim, Rivest, Suzuki, Intriligator, & Sharpe, 2000). It might be the case that the degree of convexity (or concavity) might be another basic shape dimension coded as a global unit by the rapidly adapting shape-coding mechanism perhaps mediated by IT cells.

Acknowledgements

The author is extremely grateful to observers YS and ET for their time and patience, Wilson Geisler, Marcia Grabowecky, Sania Hamilton, and the two anonymous reviewers for their constructive comments on the earlier versions of the manuscript, and the National Science Foundation (SBR-9817643) for supporting this research.

References

Berkley, M. A., Debruyn, B., & Orban, G. (1994). Illusory, motion, and luminance-defined contours interact in the human visual system. *Vision Research*, *34*(2), 209–216.

Bonds, A. B. (1991). Temporal dynamics of contrast gain in single cells of the cat striate cortex. *Visual Neuroscience*, *6*, 239–255.

Bonneh, Y., & Sagi, D. (1998). Effects of spatial configuration on contrast detection. *Vision Research*, *38*, 3541–3553.

Bowling, A., & Lovegrove, W. (1980). The effect of stimulus duration on the persistence of gratings. *Perception and Psychophysics*, *27*, 574–578.

Braddick, O., Campbell, F. W., & Atkinson, J. (1978). Channels in vision: Basic aspects. In R. Held, H. W. Leibowitz, & L.-H. Teuber (Eds.), *Handbook of sensory physiology: Vol. 8. Perception* (pp. 3–38). Berlin: Springer-Verlag.

Campbell, F. W., & Maffei, L. (1971). The tilt aftereffect: A fresh look. *Vision Research*, *11*, 833–840.

Carandini, M., Movshon, J. A., & Ferster, D. (1998). Pattern adaptation and cross-orientation interactions in the primary visual cortex. *Neuropharmacology*, *37*, 501–511.

Carlson, C. R., Moeller, J. R., & Anderson, C. H. (1984). Visual illusions without low spatial frequencies. *Vision Research*, *24*, 1407–1413.

Chelazzi, L., Duncan, J., Miller, E. K., & Desimone, R. (1998). Responses of neurons in inferior temporal cortex during memory-guided visual search. *Journal of Neurophysiology*, *80*(6), 2918–2940.

Cheng, K., Hasegawa, T., Saleem, K. S., & Tanaka, K. (1994). Comparison of neural sensitivity for stimulus speed, length, and contrast in the prestriate visual cortical areas V4 and MT of the macaque monkey. *Journal of Neurophysiology*, *71*(6), 2269–2280.

De Valois, R. L., Albrecht, D. G., & Thorell, L. G. (1982). Spatial frequency selectivity of cells in macaque visual cortex. *Vision Research*, *22*, 545–559.

Desimone, R., & Gross, C. G. (1979). Visual areas in the temporal cortex of the macaque. *Brain Research*, *178*, 363–380.

Desimone, R., & Schein, S. J. (1987). Visual properties of neurons in area V4 of the macaque: Sensitivity to stimulus form. *Journal of Neurophysiology*, *57*(3), 835–868.

Durgin, F. H., & Proffitt, D. R. (1996). Visual learning in the perception of texture: simple and contingent aftereffects of texture density. *Spatial Vision*, *9*(4), 423–474.

Field, D. J., Hayes, A., & Hess, R. F. (1993). Contour integration by the human visual system: evidence for local "association" field. *Vision Research*, *33*, 173–193.

Flanagan, P., Cavanagh, P., & Favreau, O. E. (1990). Independent orientation-selective mechanisms for the cardinal directions of color space. *Vision Research*, *30*(5), 769–778.

Foster, K. H., Gaska, J. P., Nagler, M., & Polen, D. A. (1985). Spatial and temporal frequency selectivity of neurons in visual cortical areas V1 and V2 of the macaque monkey. *Journal of Physiology*, *London*, *365*, 331–368.

Fujita, I., Tanaka, K., Ito, M., & Cheng, K. (1992). Columns for visual features of objects in monkey inferotemporal cortex. *Nature*, *360*, 343–346.

Geisler, W. S., & Albrecht, D. G. (1997). Visual cortex neurons in monkey and cats: Detection, discrimination, and identification. *Visual Neuroscience*, *14*, 897–919.

Gibson, J. J., & Radner, M. (1938). Adaptation, aftereffect and contrast in the perception of tilted lines. *Journal of Experimental Psychology*, *20*, 453–467.

Grosof, D. H., Shapley, R. M., & Hawken, M. J. (1993). Macaque V1 neurons can signal 'illusory' contours. *Nature*, *365*, 550–552.

Greenlee, M. W., & Magnussen, S. (1987). Saturation of the tilt aftereffect. *Vision Research*, *27*(6), 1041–1043.

Gross, C. G., Rocha-Miranda, C. E., & Bender, D. B. (1972). Visual properties of neurons in inferotemporal cortex of the macaque. *Journal of Neurophysiology*, *35*, 96–111.

Haenny, P. E., & Schiller, P. (1988). State dependent activity in monkey visual cortex. *Experimental Brain Research*, *69*, 225–244.

Heinze, H. J., Mangun, G. R., Burchert, W., Hinrichs, H., Scholtz, M., Munte, T. F., Gos, A., Scherg, M., Johannes, S., Hundeshagen, H., Gazzaniga, M. S., & Hillyard, S. A. (1994). Combined spatial and temporal imaging of brain activity during visual selective attention in humans. *Nature*, *372*, 543–546.

Held, R., & Shattuck, S. R. (1971). Color- and edge-sensitive channels in the human visual system: Tuning for orientation. *Science*, *174*, 314–316.

Held, R., Shattuck-Hufnagel, S., & Moskowitz, A. (1982). Color-contingent tilt aftereffect: Spatial frequency specificity. *Vision Research*, *22*, 811–817.

Hikosaka, K. (1999). Tolerances of responses to visual patterns in neurons of the posterior inferotemporal cortex in the macaque against changing stimulus size and orientation, and deleting patterns. *Behavioral Brain Research*, *100*, 67–76.

Hubel, D. H., & Wiesel, T. N. (1968). Receptive fields and functional architecture of monkey striate cortex. *Journal of Physiology*, *195*, 215–243.

Ito, M., Fujita, I., Tamura, H., & Tanaka, K. (1994). Processing of contrast polarity of visual images in inferotemporal cortex of the macaque monkey. *Cerebral Cortex*, *5*, 499–508.

Ito, M., Tamura, H., Fujita, I., & Tanaka, K. (1995). Size and position invariance of neuronal responses in monkey inferotemporal cortex. *Journal of Neurophysiology*, *73*(1), 218–226.

Kastner, S., De Weerd, P., Desimone, R., & Ungerleider, L. G. (1998). Mechanisms of directed attention in the human extrastriate cortex as revealed by functional MRI. *Science*, *282*, 108–111.

Kapadia, M. K., Ito, M., Gilbert, C. D., & Westheimer, G. (1995). Improvement in visual sensitivity by changes in local context: parallel studies in human observers and in V1 of alert monkeys. *Neuron*, *15*, 843–856.

Kim, J. S., Rivest, J., Suzuki, S., Intriligator, J. M., & Sharpe, J. A. (2000). The shape distortion effect after cerebral hemispheric lesions. *Investigative Ophthalmology and Visual Science (Suppl.)*, *41*(4), S216.

Komatsu, H., Ideura, Y., Kaji, S., & Yamane, S. (1992). Color selectivity of neurons in the inferior temporal cortex of the awake macaque monkey. *Journal of Neuroscience*, *12*(2), 408–424.

Lamme, V. A., Van Dijk, B. W., & Spekreijse, H. (1993a). Organization of texture segregation processing in primate visual cortex. *Visual Neuroscience*, *10*(5), 781–790.

Lamme, V. A., Van Dijk, B. W., & Spekreijse, H. (1993b). Contour from motion processing occurs in primary visual cortex. *Nature*, *363*, 541–543.

Lee, C., Rohrer, W. H., & Sparks, D. L. (1988). Population coding of saccadic eye movements by neurons in the superior colliculus. *Nature*, *332*, 357–360.

Leventhal, A. G., Wang, Y., Schmolesky, M. T., & Zhou, Y. (1998). Neural correlates of boundary perception. *Visual Neuroscience*, *15*, 1107–1118.

Luck, S. J., Chelazzi, L., Hillyard, S., & Desimone, R. (1997). Neural mechanisms of spatial selective attention in areas V1, V2, and V4 of macaque visual cortex. *Journal of Neurophysiology*, *77*, 24–42.

Logothetis, N. K., & Sheinberg, D. L. (1996). Visual object recognition. *Annual Review of Neuroscience*, *19*, 577–621.

Lueschow, A., Miller, E. K., & Desimone, R. (1994). Inferior temporal mechanisms for invariant object recognition. *Cerebral Cortex*, *5*, 523–531.

Magnussen, S., & Kurtenbach, W. (1980). Linear summation of tilt illusion and tilt aftereffect. *Vision Research*, *20*, 39–42.

Magnussen, S., & Kurtenbach, W. (1979). A test for contrast-polarity selectivity in the tilt aftereffect. *Perception*, *8*, 523–528.

Mangun, G. R., Hillyard, S. A., & Luck, S. J. (1993). Electrocortical substrates of visual selective attention. In D. Meyer, & S. Kornblum, *Attention and performance XIV* (pp. 219–243). Cambridge, MA: MIT Press.

McAdams, C. J., & Maunsell, J. H. R. (1999). Effects of attention on orientation-tuning functions of single neurons in macaque cortical area V4. *Journal of Neuroscience*, *19*(1), 431–441.

Meese, T. S., & Georgeson, M. A. (1996). The tilt aftereffect in plaids and gratings: channel codes, local signs, and "patchwise" transforms. *Vision Research*, *36*(10), 1421–1437.

Miller, E. K., Li, L., & Desimone, R. (1993). Activity of neurons in anterior inferior temporal cortex during a short-term memory task. *Journal of Neuroscience*, *13*(4), 1460–1478.

Mishkin, M., Ungerleider, L. G., & Macko, K. A. (1983). Object vision and spatial vision: Two central pathways. *Trends in Neuroscience*, *6*, 414–417.

Mitchell, D. E., & Muir, D. W. (1976). Does the tilt after-effect occur in the oblique meridian? *Vision Research*, *16*, 609–613.

Moran, J., & Desimone, R. (1985). Selective attention gates visual processing in the extrastriate cortex. *Science*, *229*, 782–784.

O'Shea, R. P., Wilson, R. G., & Duckett, A. (1993). The effects of contrast reversal on the direct, indirect, and interocularly-transferred tilt aftereffect. *New Zealand Journal of Psychology*, *22*(2), 94–100.

O'Toole, B., & Wenderoth, P. (1977). The tilt illusion: Repulsion and attraction effects in the oblique meridian. *Vision Research*, *17*, 367–374.

Ohzawa, I., Sclar, G., & Freeman, R. D. (1985). Contrast gain control in the cat's visual system. *Journal of Neurophysiology*, *54*(3), 651–667.

Paradiso, M. A., Shimojo, S., & Nakayama, K. (1989). Subjective contours, tilt aftereffects, and visual cortical organization. *Vision Research*, *29*(9), 1205–1213.

Peterhans, E., & von der Heydt, R. (1991). Subjective contours—bridging the gap between psychophysics and physiology. *Trends in Neuroscience*, *14*, 112–119.

Peterhans, E., von der Heydt, R., & Baumgartner, G. (1986). Neural responses to illusory contour stimuli reveal stages of visual cortical processing. In J. D. Pettigrew, K. J. Sanderson, & W. R. Levick, *Visual neuroscience* (pp. 343–351). Cambridge: Cambridge University Press.

Polat, U., & Norcia, A. M. (1996). Neurophysiological evidence for contrast dependent long-range facilitation and suppression in the human visual cortex. *Vision Research*, *36*(14), 2099–2109.

Polat, U., & Sagi, D. (1993). Lateral interactions between spatial channels: suppression and facilitation revealed by lateral masking experiments. *Vision Research*, *33*, 993–999.

Regan, D., & Hamstra, S. J. (1992). Shape discrimination and the judgment of perfect symmetry: Dissociation of shape from size. *Vision Research*, *32*, 1845–1864.

Reynolds, J. H., Chelazzi, L., & Desimone, R. (1999). Competitive mechanisms subserve attention in macaque areas V2 and V4. *Journal of Neuroscience*, *19*(5), 1736–1753.

Rijsdijk, J. P., Kroon, J. N., & van der Wildt, G. J. (1978). Contrast sensitivity as a function of position on the retina. *Vision Research*, *20*, 235–241.

Rivest, J., Intriligator, J. M., Suzuki, S., & Warner, J. (1998). A shape distortion effect that is size invariant. *Investigative Ophthalmology and Visual Science (Suppl.)*, *39*(4), S853.

Rivest, J., Intriligator, J. M., Warner, J., & Suzuki, S. (1997). Color and luminance combine at a common neural site for shape distortions. *Investigative Ophthalmology and Visual Science (Suppl.)*, *38*(4), S1000.

Roelfsema, P. R., Lamme, V. A. F., & Spekreijse, H. (1998). Object-based attention in the primary visual cortex of the macaque monkey. *Nature*, *395*, 376–381.

Rolls, E. T., & Baylis, G. C. (1986). Size and contrast have only small effects on the responses to faces of neurons in the cortex of the superior temporal sulcus of the monkey. *Experimental Brain Research*, *65*, 38–48.

Rubin, N., Nakayama, K., & Shapley, R. (1996). Enhanced perception of illusory contours in the lower versus upper visual hemifields. *Science*, *271*, 651–653.

Sary, G., Vogels, R., Kovacs, G., & Orban, G. A. (1995). Responses of monkey inferior temporal neurons to luminance-, motion, and texture-defined gratings. *Journal of Neurophysiology*, *73*(4), 1341–1354.

Sato, T., Kawamura, T., & Iwai, E. (1980). Responsiveness of inferotemporal single units to visual pattern stimuli in monkeys performing discrimination. *Experimental Brain Research*, *38*, 313–319.

Saul, A. B., & Cynader, M. S. (1989). Adaptation in single units in visual cortex: The tuning of aftereffects in the spatial domain. *Visual Neuroscience*, *2*, 593–607.

Sclar, G., Lennie, P., & DePriest, D. D. (1989). Contrast adaptation in striate cortex of macaque. *Vision Research*, *29*(7), 747–755.

Sclar, G., Maunsell, J. H. R., & Lennie, P. (1990). Coding of image contrast in central visual pathways of the macaque monkey. *Vision Research*, *30*(1), 1–10.

Sekuler, R., & Littlejohn, J. (1974). Tilt aftereffect following very brief exposures. *Vision Research*, *14*, 151–152.

Sheth, B. R., Sharma, J., Rao, S. C., & Sur, M. (1996). Orientation maps of subjective contours in visual cortex. *Science*, *274*, 2110–2115.

Spitzer, H., Desimone, R., & Moran, J. (1988). Increased attention enhances both behavioral and neuronal performance. *Science*, *240*, 338–340.

Spivey, M. J., & Spirn, M. J. (2000). Selective visual attention modulates the direct tilt aftereffect. *Perception and Psychophysics*, *62*(8), 1525–1533.

Suzuki, S. (1999). Influences of contexts on a non-retinotopic skew-contrast effect. *Investigative Ophthalmology and Visual Science (Suppl.)*, *40*(4), S812.

Suzuki, S., & Cavanagh, P. (1997). Focused attention distorts visual space: An attentional repulsion effect. *Journal of Experimental Psychology: Human Perception and Performance*, *23*, 443–463.

Suzuki, S., & Cavanagh, P. (1998). A shape-contrast effect for briefly presented stimuli. *Journal of Experimental Psychology: Human Perception and Performance*, *24*(5), 1315–1341.

Suzuki, S., & Grabowecky, M. (2000). Attention during adaptation weakens negative afterimages. *The 41st annual meeting of the Psychonomic Society*. New Orleans, LA.

Suzuki, S., & Rivest, J. (1998). Interactions among "aspect-ratio channels. *Investigative Ophthalmology and Visual Science (Suppl.)*, *39*(4), S855.

Tanaka, K. (1996). Inferotemporal cortex and object vision. *Annual Review of Neuroscience*, *19*, 109–139.

Ts'o, D. Y., & Gilbert, C. D. (1988). The organization of chromatic and spatial interactions in the primate striate cortex. *Journal of Neuroscience*, *8*(5), 1712–1727.

Ts'o, D., & Roe, A. W. (1995). Functional compartments in visual cortex: segregation and interaction. In M. S. Gazzaniga, *The cognitive neurosciences* (pp. 325–337). Cambridge, MA: MIT Press.

Turvey, M. T. (1978). Visual processing and short-term memory. In W. K. Estes (Ed.), *Handbook of learning and cognitive processes: Vol. 5. Human information processing* (pp. 91–142). Hillsdale, NJ: Erlbaum.

Tyler, C. W. (1975). Stereoscopic tilt and size aftereffects. *Perception*, *4*, 187–192.

Ungerleider, L. G., & Mishkin, M. (1982). Two cortical visual systems. In D. J. Ingle, M. A. Goodale, & R. J. W. Mansfield, *Analysis of visual behavior* (pp. 549–586). Cambridge, MA: MIT Press.

van der Zwan, R., & Wenderoth, P. (1995). Mechanisms of purely subjective contour tilt aftereffects. *Vision Research*, *35*(18), 2547–2557.

Vogels, R., & Orban, G. A. (1994). Activity of inferior temporal neurons during orientation discrimination with successively presented gratings. *Journal of Neurophysiology*, *71*(4), 1428–1451.

Vogels, R., Sary, G., & Orban, G. A. (1995). How task-related are the responses of inferior temporal neurons? *Visual Neuroscience*, *12*, 207–214.

Wade, N. J. (1980). The influence of color and contour rivalry on the magnitude of the tilt illusion. *Vision Research*, *20*, 229–233.

Ware, C., & Mitchell, D. E. (1974). The spatial selectivity of the tilt aftereffect. *Vision Research*, *14*, 735–737.

Wenderoth, P., & Johnstone, S. (1987). Possible neural substrates for orientation analysis and perception. *Perception*, *16*, 693–709.

Wenderoth, P., & van der Zwan, R. (1989). The effects of exposure duration and surrounding frames on direct and indirect tilt aftereffects and illusions. *Perception and Psychophysics*, *46*(4), 338–344.

Wilson, H. R., & Humanski, R. (1993). Spatial frequency adaptation and contrast gain control. *Vision Research*, *33*, 1133–1149.

Wolfe, J. M. (1984). Short test flashes produce large tilt aftereffects. *Vision Research*, *24*(12), 1959–1964.

Wolfe, J. M., & Held, R. (1982). Gravity and the tilt aftereffect. *Vision Research*, *22*, 1075–1078.